

Average Star Formation Parameters in the Local Volume of the Universe

I. D. Karachentsev^{1,*} and A. A. Popova²

¹*Special Astrophysical Observatory, Russian Academy of Sciences, Nizhnii Arkhyz, 369167 Russia*

²*Peter the Great St. Petersburg Polytechnic University, Saint Petersburg, 195251 Russia*

Based on the fluxes of 1400 nearby galaxies observed in far ultraviolet (FUV) and in the H α line, we determined the global star formation rate per unit Universe volume, $j_{\text{SFR}} = (1.34 \pm 0.16) 10^{-2} M_{\odot} \text{yr}^{-1} \text{Mpc}^{-3}$. With the current star formation rate (SFR), $(65 \pm 4)\%$ of the observed stellar mass is reproduced in the cosmological time of 13.8 billion years. The neutral gas reserves in the Local Volume with a radius of 11 Mpc will facilitate the current SFR on a scale of approximately another 5 billion years.

Keywords: galaxies—star formation: galaxies—evolution

1. INTRODUCTION

The integral rate of star formation in the galaxy, SFR , expressed in units of solar masses per year ($M_{\odot} \text{yr}^{-1}$), is one of the most important characteristics of gas transformation into stars. The specific star formation rate per unit stellar mass, $sSFR = SFR/M_*$, differs for active and passive galaxies by a factor of 10^4 – 10^6 . The mean star formation rate density in a cubic megaparsec, j_{SFR} , determines the intensity of the cosmic evolution of the Universe. According to multiple observational data (Madau et al., 1998; Madau and Dickinson, 2014), the value of j_{SFR} in the consequential volume of the Universe increases with decreasing redshift z from $z \simeq 6$ to $z \simeq 2$ and then drops by an order of magnitude toward the current epoch, $z = 0$. In order to model the star formation process and describe the $j_{\text{SFR}}(z)$ dependences, one needs to fix the zero point value, $j_{\text{SFR}}(0)$, as accurately as possible. This task is the main aim of our work.

To determine the SFR of a galaxy, the H α Balmer line integral flux is usually used. According to Kennicutt (1998) and Lee et al. (2009b),

$$\log SFR = 8.98 + 2 \log D + \log F_c(\text{H}\alpha),$$

where the distance D to a galaxy is expressed in Mpc, and the H α line flux is in $\text{erg cm}^{-2} \text{s}^{-1}$ and corrected with account for extinction in the Milky Way and in the galaxy itself. The details of taking into account the internal and external extinction are described in Lee et al. (2009b).

Another method of estimating SFR is based on measuring the flux from a galaxy in the far ultraviolet (FUV, $\lambda_{\text{eff}} = 1539 \text{ \AA}$, $FWHM = 269 \text{ \AA}$) using the relation

$$\log SFR = 2.78 + 2 \log D - 0.4m_{\text{FUV}}^c,$$

where D is the distance in Mpc and m_{FUV}^c is the apparent FUV-band magnitude of the galaxy corrected for internal and external extinction (Lee et al., 2011). The ultraviolet sky survey carried out with the GALEX satellite serves as the main source of the m_{FUV} magnitude data (Martin et al., 2005; Gil de Paz et al., 2007).

In addition to these two methods, SFR estimates were made from the infrared flux of a galaxy in the assumption that the FUV-flux of the stellar population is absorbed by interstellar dust and re-emitted in the infrared range.

2. ESTIMATES OF THE STAR FORMATION RATE DENSITY IN THE CURRENT EPOCH

Attempts to determine $j_{\text{SFR}}(0)$ from the data on nearby galaxies were undertaken by many authors. Gallego et al. (1995) used for this purpose the H α -flux values for 264 galaxies with H α line equivalent widths larger than 10 \AA and redshifts $z < 0.045$. Independent H α -flux estimates for several hundred nearby galaxies were made by Pérez-González et al. (2003) and James et al. (2008). Hanish et al. (2006) used the equivalent widths $EW(\text{H}\alpha)$ to determine j_{SFR} for a sample of 468 galaxies with $z < 0.04$ observed in the HI neutral hydrogen line in the HIPASS

* idkarach@gmail.com

Table 1. Estimates of the mean star formation rate density in the current epoch

$j_{\text{SFR}}(0) \times 10^{-2}$	Data	N	z	Δ	Reference
(1)	(2)	(3)	(4)	(5)	(6)
1.3 ± 0.2	H α , $EW > 10 \text{ \AA}$	264	< 0.045	-0.04	Gallego et al. (1995)
2.2 ± 0.7	H α	191	0.026	-0.03	Pérez-González
1.5 ± 0.2	H α , SDSS	$\sim 100\,000$	0.11	-0.12	Brinchmann et al. (2004)
1.1 ± 0.3	FUV	896	< 0.10	-0.06	Wyder et al. (2005)
1.5 ± 0.3	H α , HIPASS	468	< 0.04	-0.03	Hanish et al. (2006)
1.6 ± 0.2	FUV, SDSS	$\sim 50\,000$	~ 0.10	-0.06	Salim et al. (2007)
1.9 ± 0.2	H α , SDSS	327	0.01	-0.01	James et al. (2008)
1.9 ± 0.3	FUV, SDSS	$\sim 50\,000$	< 0.10	-0.06	Robotham and Driver (2011)
1.4 ± 0.3	FUV, H α	869	0.001	0.00	Karachentsev et al. (2013)
1.34 ± 0.16	FUV, H α	1428	0.001	0.00	This work

survey. Brinchmann et al. (2004) presented the j_{SFR} estimated based on $N \sim 10^5$ galaxies with an average redshift of $\langle z \rangle = 0.11$ from the SDSS optical sky survey (Abazajian et al., 2009).

Wyder et al. (2005) determined the local SFR density from FUV fluxes of 896 galaxies with $z < 0.10$. Salim et al. (2007) and Robotham and Driver (2011) used for this purpose the FUV-fluxes of a large number of galaxies from the SDSS survey with redshifts of $z < 0.10$.

Such estimations were usually accompanied by certain expectations about the shape of the luminosity function of the galaxy sample considered and other model assumptions. An uncertainty about the size of the volume to which the measured FUV-fluxes pertain has arisen during the j_{SFR} density calculation. The method used by Karachentsev et al. (2013) for estimating $j_{\text{SFR}}(0)$ from the Local Volume galaxies with distances of $D < 11$ Mpc suffered the least from this limitation. A summary of the local star formation rate density from various sources is presented in Table 1.

Its columns contain: (1)—star formation rate density in units of $10^{-2} M_{\odot} \text{ yr}^{-1} \text{ Mpc}^{-3}$ corrected to $z=0$ for the Hubble parameter $H_0 = 70 \text{ km s}^{-1} \text{ Mpc}^{-1}$ with the standard error indicated; (2)—the nature of the used data; (3)—the number of galaxies in the sam-

ple; (4)—the redshift mean value and interval; (5)— $z = 0$ correction in the density logarithm $\Delta \log(j_{\text{SFR}})$ in an assumption that the $j_{\text{SFR}}(z)/j_{\text{SFR}}(0) \simeq (1+z)^{2.7}$ dependence is true for $z \ll 1$ according to Madau and Dickinson (2014); (6)—reference to the observational data source.

The data presented above demonstrates that the difference between some average star formation rate density estimates in the current epoch reaches a factor of 2.

3. SAMPLE OF LOCAL VOLUME (LV) GALAXIES

The list of nearby galaxies with expected distances not exceeding 11 Mpc has been replenishing quickly in the recent years due to the emergence of deeper optical and HI-surveys of large areas of the sky. While the Catalog of Neighboring Galaxies (Karachentsev et al., 2004) included $N = 450$ galaxies, in the Updated Nearby Galaxy Catalog (UNGC, Karachentsev et al., 2013), their number has increased to $N = 869$. Observational data on the Local Volume galaxies are presented online at <http://www.sao.ru/lv/lv gdb> and described in Kaisina et al. (2012). Distances were measured for more than half of

the sample galaxies with the Hubble Space Telescope, at an accuracy of about 5%. The most complete summary of the distances is presented in the Extragalactic Distance Database = EDD (Anand et al., 2021). The online version of the UNGC catalog is regularly updated by new objects and new data on the nearby galaxies. Currently, the number of suggested Local Volume members exceeds 1400 objects.

A significant portion of these galaxies have the $H\alpha$ - and FUV-fluxes measured. When determining the integral star formation rate of a galaxy, we preferred FUV-flux data, since the SFR estimates based on these data relate to a typical time interval of about 100 million years, whereas the $H\alpha$ -flux of a galaxy characterizes the SFR on a shorter scale of about 10 million years. We used the $SFR(H\alpha)$ estimates for galaxies with no FUV-flux data. Usually this applied to objects at low galactic latitudes, where the FUV-range extinction is especially high.

Note that the $SFR(H\alpha)$ and $SFR(FUV)$ estimates are mutually well-calibrated for the case of spiral galaxies. When transitioning from massive galaxies to dwarfs, the dispersion of the $SFR(H\alpha)/SFR(FUV)$ ratio increases with decreasing stellar mass of a galaxy, and the average value of this ratio plummets approximately by a factor of three for the least massive objects (Lee et al., 2009a; Karachentsev and Kaisina, 2019).

Along with the SFR values for the Local Volume galaxies, the online version of the UNGC contains data on the stellar masses M_* and masses of neutral hydrogen M_{HI} in these galaxies. Both these parameters are the main integral markers of the gas-to-stars transformation process.

4. STAR FORMATION RATE IN THE LOCAL VOLUME

The distribution of LV galaxies by integral star formation rate and distance within 12 Mpc is presented in Fig. 1. Galaxies with $SFR(FUV)$ estimates are shown by stars, and objects with SFR measured only by $H\alpha$ -flux are shown by crosses. FUV and $H\alpha$ -flux data are missing for 170 sample galaxies. The SFR estimates

for these galaxies are made by calibration dependences between SFR and M_* , constructed for galaxies of various morphological types (presented below in Section 5). These galaxies are shown in Fig. 1 by the empty circles.

About a quarter of the LV galaxies have only the upper FUV-flux estimates available. Most of them are dwarf spheroidal galaxies (dSph) with no noticeable gas stored for star formation. We attributed to them the SFR value corresponding to the upper limit of the FUV-flux. These faint objects form a narrow sequence in the lower part of Fig. 1 near $SFR = 10^{-5}$. Taking these galaxies into account or ignoring them changes the average SFR density estimate in the LV by only a fraction of a percent.

For the most extended galaxies, the Milky Way (MW) and Andromeda (M31), FUV-fluxes were taken from Chomiuk and Povich (2011) and Rahmani et al. (2016) correspondingly. Evidently, the LV hosts 10 galaxies with star formation rates higher than in our Galaxy.

The brightest star formation source is in the spiral galaxy NGC 4631, which reproduces about $5 M_\odot$ per year. At $D > 10$ Mpc distances the SFR data density drops rapidly, which points to the incompleteness of the sample at the far LV boundary.

5. SPECIFIC STAR FORMATION RATE IN LV GALAXIES

Determining the specific star formation rate of a galaxy $sSFR = SFR/M_*$ presumes the knowledge of its total stellar mass. However, thorough integral mass estimates are known for only a few nearby galaxies. Calculating them requires using different model assumptions, in particular, about the form of the initial stellar mass function. A simplified method of estimating M_* is based on the data on integral galaxy luminosity, preferably in the K -band, where the effects of internal light extinction and bursts of star formation are minimal.

The UNGC catalog (Karachentsev et al., 2013) contains data on the luminosity of galaxies in the K -band, L_K , measured in the 2MASS-survey of the entire sky (Jarrett et

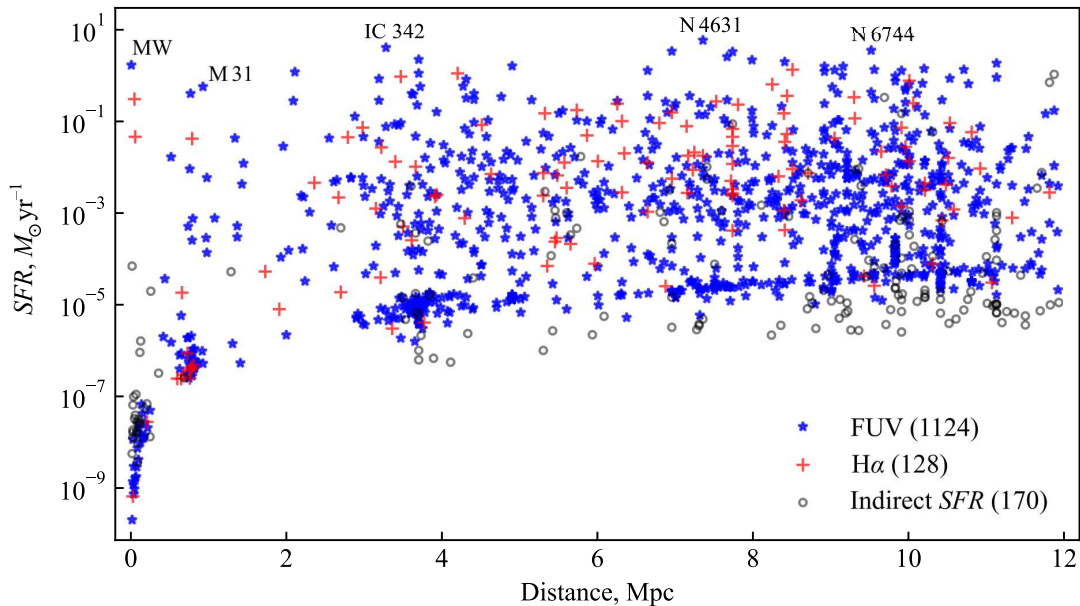


Figure 1. Distribution of the Local Volume galaxies by integral star formation rate SFR and distance. Galaxies with SFR estimates based on the FUV-flux are shown by stars, those with estimates from the $H\alpha$ -flux are shown by crosses, and objects with indirect SFR estimates by the calibration dependence are marked by empty circles.

al., 2000; Skrutskie et al., 2006) or estimated from the luminosity of a galaxy in other bands. To determine M_* we used the relation $M_*/L_K = 0.6 M_\odot/L_\odot$, justified by Lelli et al. (2016). The proportionality coefficient 0.6 depends weakly on the morphological type of a galaxy and was neglected.

The distribution of LV galaxies by stellar mass and distance is presented in Fig. 2a. The same symbols as in Fig. 1 are used. Evidently, the LV includes 22 galaxies with masses exceeding the stellar mass of the Milky Way and M31. The most massive representatives of the LV are NGC 4594 (“Sombrero”) and Maffei 2, relating to the early types with suppressed star formation.

Figure 2b shows the distribution of LV galaxies by specific star formation rate and distance. The designations of galaxies with different SFR data sources are the same as in the upper panel.

The highest star formation rates per unit stellar mass are demonstrated by the dwarf galaxies (NGC 1592, AGC 124635, Mrk 036) in an active phase (burst) of star formation. The diagram shows horizontal sequences of “active” galaxies ($sSFR \sim 10^{-10} \text{ yr}^{-1}$), “passive” galaxies ($sSFR \sim 10^{-12} \text{ yr}^{-1}$) with the so-called “green valley” between them.

The vertical “columns” in Fig. 2 correspond to groups of galaxies where the distances of some faint members are identified with the distance to the main galaxy.

Figure 3 shows the distribution of spiral and irregular galaxies with morphological types $T = 2-10$ on the de Vaucouleurs scale by integral star formation rate and integral stellar mass. The linear regression there, $\log SFR = 1.02 \log M_* - 10.30$, was used to estimate the SFR in galaxies without FUV- and $H\alpha$ -fluxes, which are shown by the empty circles in the previous figures. A similar calibration dependence, $\log SFR = 0.86 \log(M_*) - 10.80$, was constructed for passive galaxies ($T < 2$) in order to account for their very small contribution to the total SFR of the Local Volume.

6. SFR DENSITY IN THE LOCAL VOLUME

Summing up the SFR values for individual galaxies and dividing the sum by volume $(4\pi/3)D^3$, we obtain the distribution of the mean star formation rate density within the distance D , shown in Fig. 4a. The density $j_{SFR}(D)$ drops with increasing D for two rea-

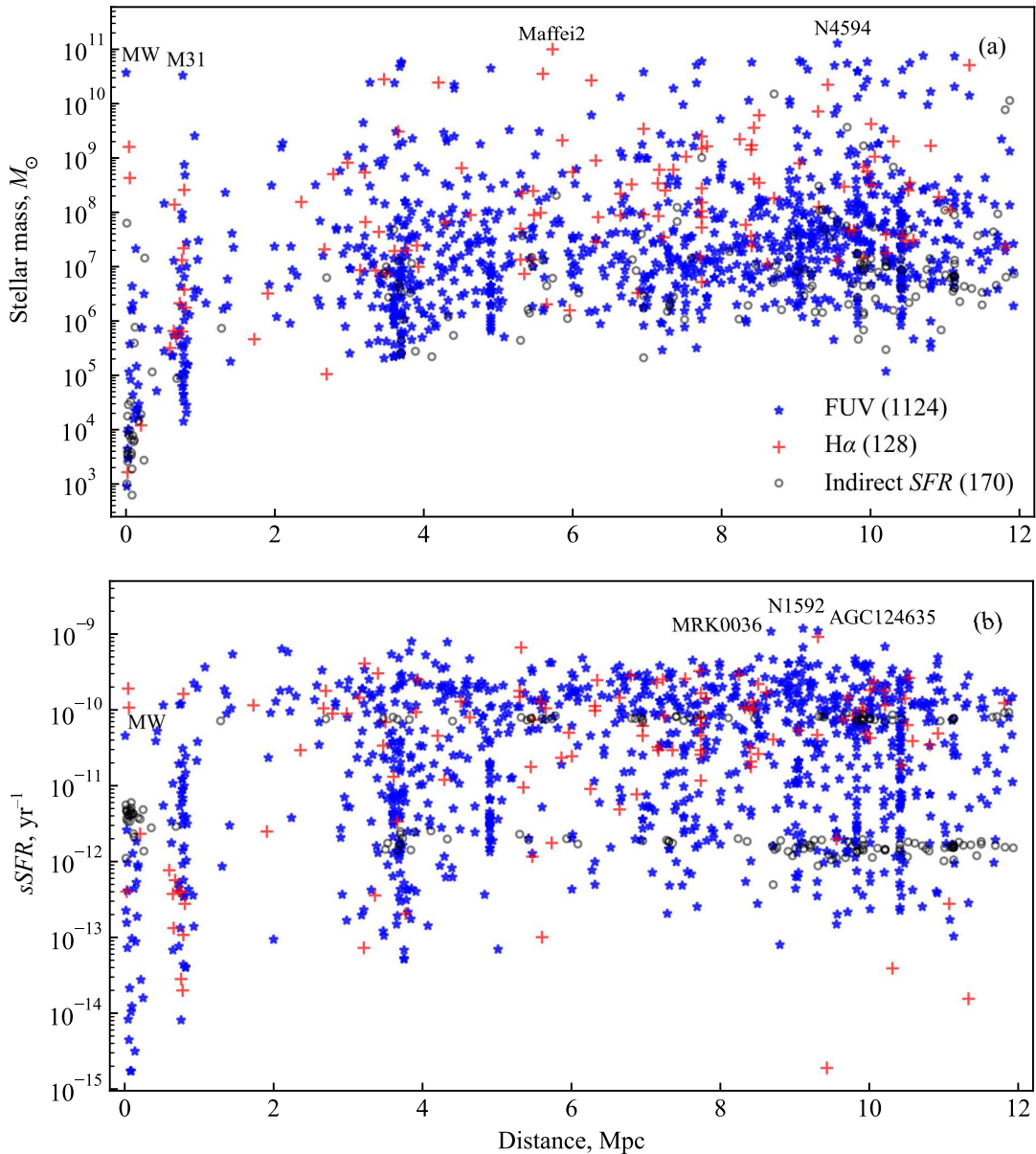


Figure 2. Panel (a)—distribution of the Local Volume galaxies by stellar mass and distance. Panel (b)—distribution of the same galaxies by specific star formation rate. The symbols are the same as in Fig. 1.

sons. First, we are located inside the Local Group, which is surrounded by several other groups (M 81, NGC 253, Centaurus A) at a distance of about 4 Mpc. Second, the completeness of the sample decreases near the sample boundary at $D \gtrsim 10$ Mpc due to the missed galaxies whose distances remain unmeasured. The upper polygonal line shows the contribution of all LV galaxies with account for the 170 galaxies with no measured FUV- and $H\alpha$ -fluxes. The contribution of these mostly small galaxies is noticeable only at the far LV boundary.

Figure 4b shows the distribution of the average stellar mass density j_{M_*} in the LV. Evidently, the $j_{\text{SFR}}(D)$ and $j_{M_*}(D)$ distributions behave in a similar manner. The horizontal stripe near the lower edge of the panel corresponds to the average global stellar density $j_{M_*} = (2.6 \pm 0.1) \times 10^8 M_\odot \text{Mpc}^{-3}$, obtained from the Driver et al. (2012) data regarding the K -luminosity global density, $(4.3 \pm 0.2) \times 10^8 L_\odot \text{Mpc}^{-3}$, for $M_*/L_K = 0.6 M_\odot/L_\odot$. The observed distribution of stellar density in the LV is higher than the global value

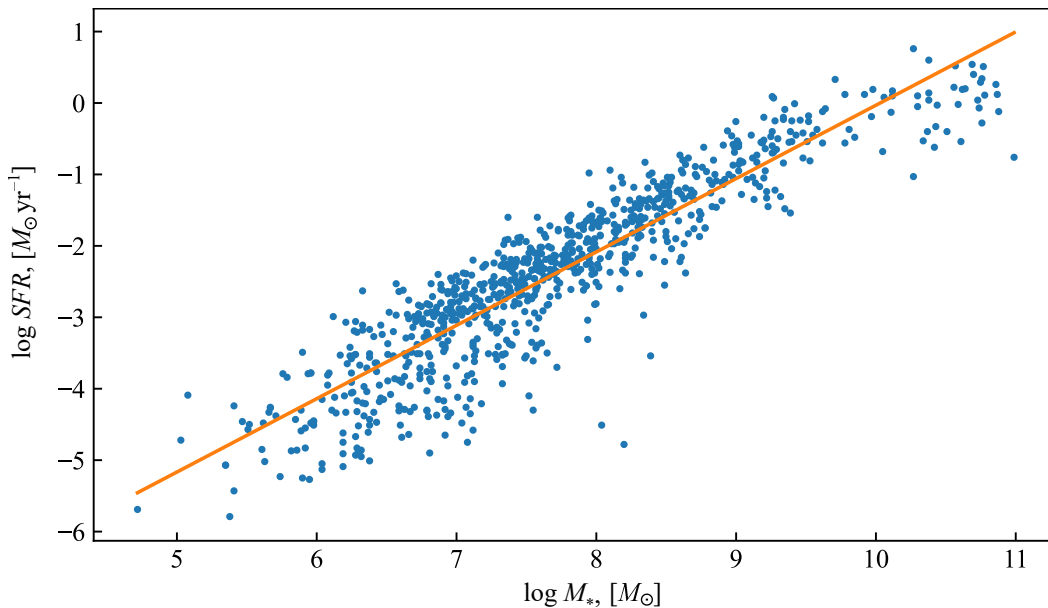


Figure 3. Relation between the integral star formation rate and stellar mass for late-type Local Volume galaxies ($T = 2-10$).

on all scales. According to the data obtained by Karachentsev and Telikova (2018), the excess of the observed local stellar density in an 11 Mpc radius volume amounts to a factor of (1.46 ± 0.10) and becomes insignificant at $D \simeq 40$ Mpc.

Figure 4c replicates the behavior of the mean specific star formation rate with increasing distance D . The variations of j_{sSFR} with increasing volume are relatively small.

We adopted $\langle j_{\text{sSFR}} \rangle = (4.7 \pm 0.3) 10^{-11} \text{ yr}^{-1}$ as the mean value. Therefore, given this average star formation rate, the Local Volume reproduces $(65 \pm 4)\%$ of its observed stellar mass over the cosmological time of 13.8 billion years.

7. AVERAGE DENSITY OF NEUTRAL GAS IN THE LOCAL VOLUME

Surveys of large areas of the sky in the neutral hydrogen HI line at $\lambda = 21$ cm (HIPASS, Koribalski et al., 2004; ALFALFA, Haynes et al., 2011), as well as dedicated observations of individual galaxies in HI (Huchtmeier et al., 2000) led to the discovery of an HI-flux, F_{HI} , in most of the nearby galaxies.

According to Roberts and Haynes (1994), the mass of neutral gas in a galaxy is expressed through F_{HI} as $M_{\text{gas}} = 1.4 \times 2.36 \times 10^5 D^2 F_{\text{HI}}$,

where D is measured in Mpc, F_{HI} is in Jy km s^{-1} , and the 1.4 factor accounts for the contribution of heavier elements to the gas mass.

The panels in Fig. 5 show the relation between the gas mass and stellar mass in early type galaxies ($T < 2$) and in spiral and irregular galaxies with morphological types $T = (2-10)$.

These calibration dependences with linear regressions $\log M_{\text{gas}} = 0.78 \log M_* + 0.80$ for $T < 2$ and $\log M_{\text{gas}} = 0.72 \log M_* + 2.30$ for $T = (2-10)$ were used to estimate the mass of the gas in the LV galaxies that were not covered by the HI observations. This primarily relates to northern sky galaxies with declinations $\text{Dec} > +39^\circ$, located beyond the HIPASS and ALFALFA survey limits. The regression lines in both panels show that the M_{gas}/M_* ratio increases from massive galaxies to dwarfs, indicating a slower (dormant) star formation process in dwarf systems.

The distribution of LV galaxies by gas mass and distance is presented in Fig. 6. Only half of the LV galaxies (720 out of 1422) have direct HI-flux measurements. For the remaining 492 galaxies (shown by open circles) the gas mass estimates were made using the calibration dependences in Fig. 5. The objects richest in gas are the spiral Sc-galaxies NGC 6744, IC 342, NGC 6946.

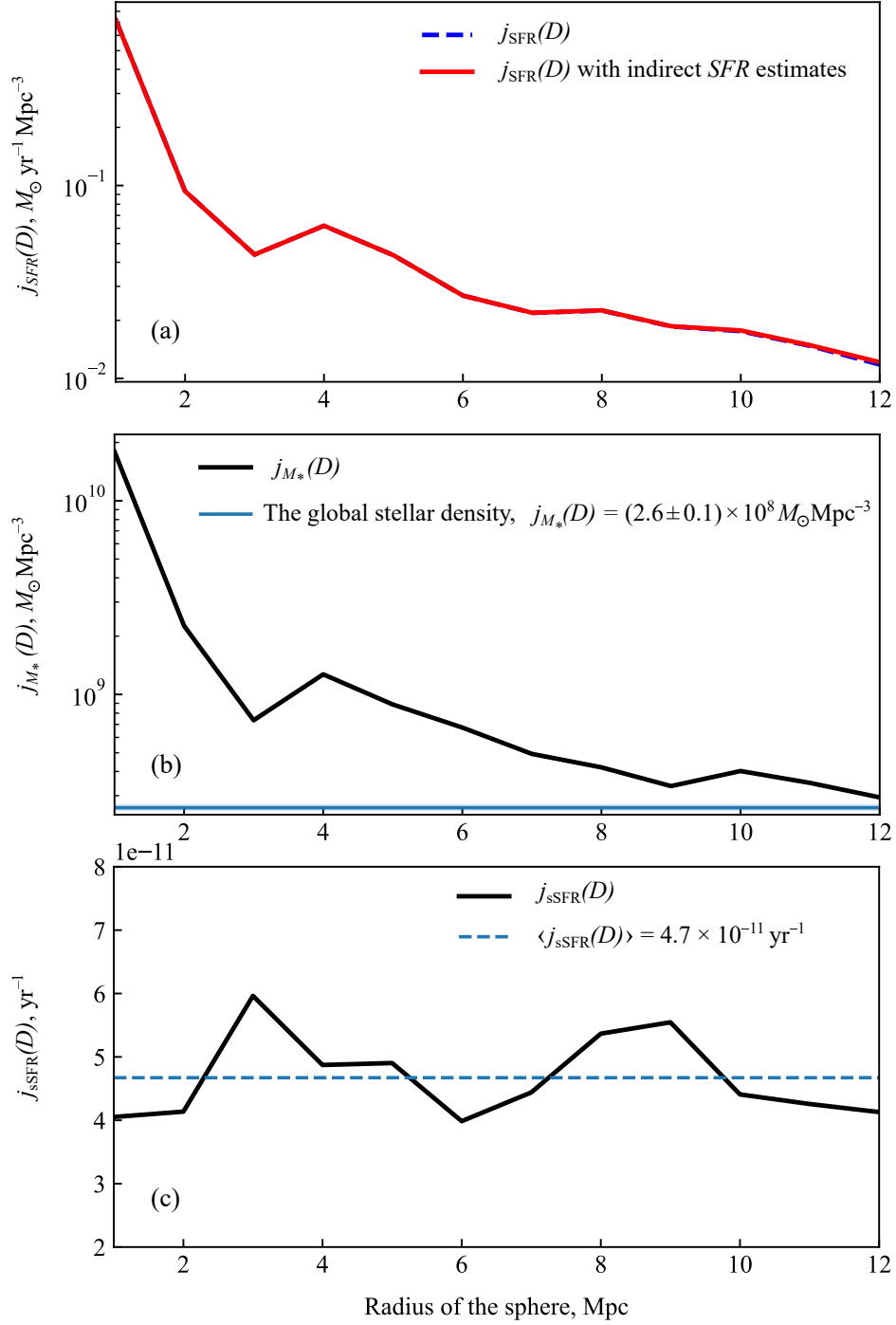


Figure 4. Panel (a)—mean star formation density in the Local Volume spheres of different radii D . Panel (b)—mean stellar mass density in the Local Volume spheres. The horizontal stripe near the lower edge corresponds to the global stellar density. Panel (c)—distribution of the specific star formation rate in the Local Volume.

Figure 7a shows the distribution of the average neutral gas mass density in D Mpc radius spheres. The lower polygonal line shows the dependence with account for only the direct HI-flux estimates. The upper line is plotted for the

entire galaxy sample, including cases with gas mass estimates made by the calibration dependences in Fig. 5. The contribution of these unobserved galaxies to the total gas density turned out to be small.

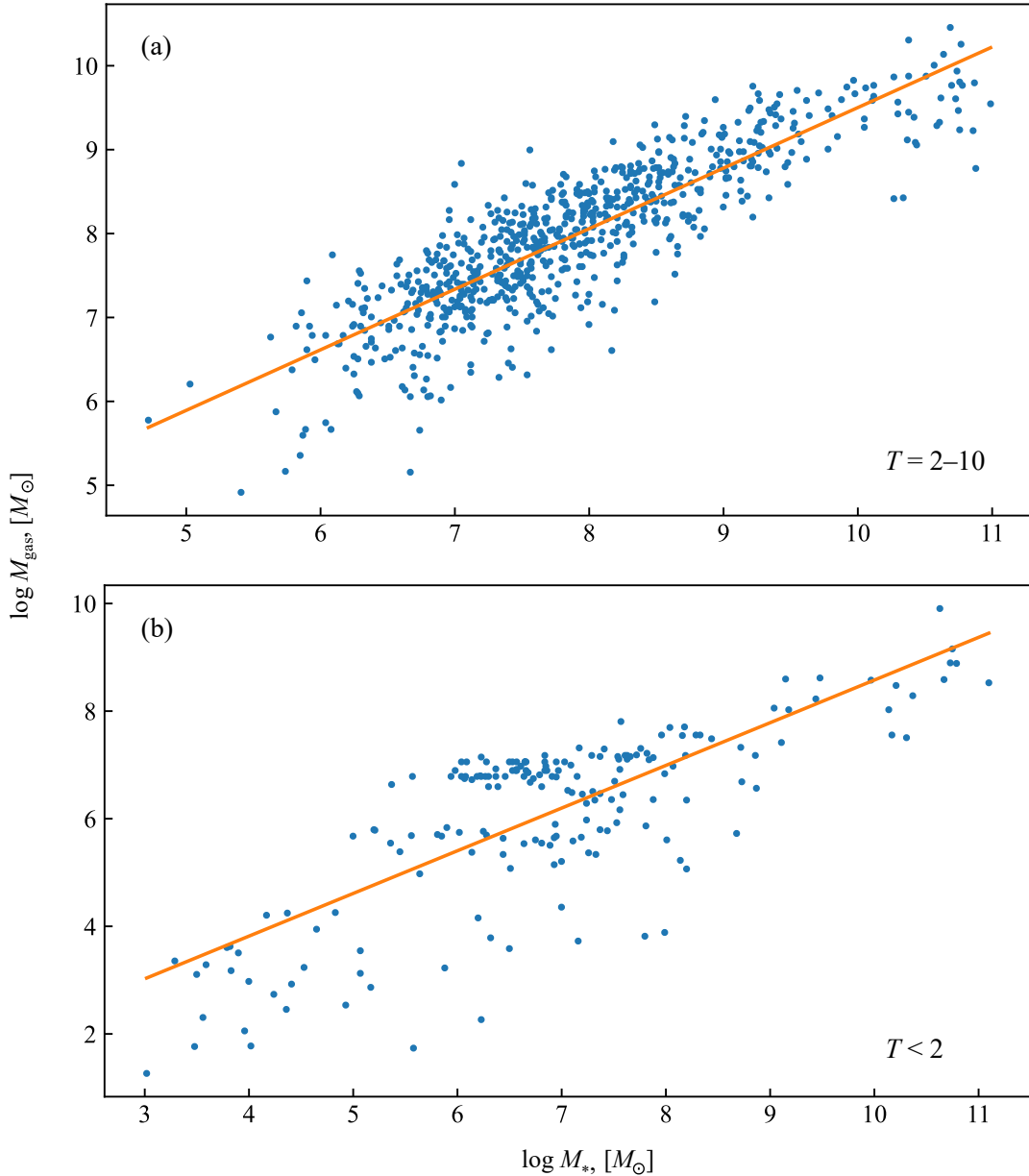


Figure 5. Relation between the gas mass and stellar mass for late-type $T = [2-10]$ (a) and early-type galaxies $T < 2$ (b).

The total gas-to-stellar mass ratio for galaxies inside spheres of different radii is presented in Fig. 7b. The typical average gas-to-stars density ratio in the LV is approximately 0.24. Therefore, the available stock on neutral gas in the LV can maintain the observed star formation rate in it on a scale of another 5 billion years. We should note, however, that according to the Zhou et al. (2023) data, roughly half of the neutral gas in the galaxies can be below the sensitivity limit of the carried out HI-surveys.

The small value of the M_{gas}/M_{*} ratio indi-

cates that the star formation process in the Local Volume is already fading, nearing its completion.

8. DISCUSSION AND CONCLUDING REMARKS

The data on the SFR , M_{*} and M_{gas} density presented in Fig. 4 and Fig. 7 were obtained in the assumption of a homogeneous distribution of LV galaxies on the celestial sphere. At the same time, the number of galaxies in the sine inter-

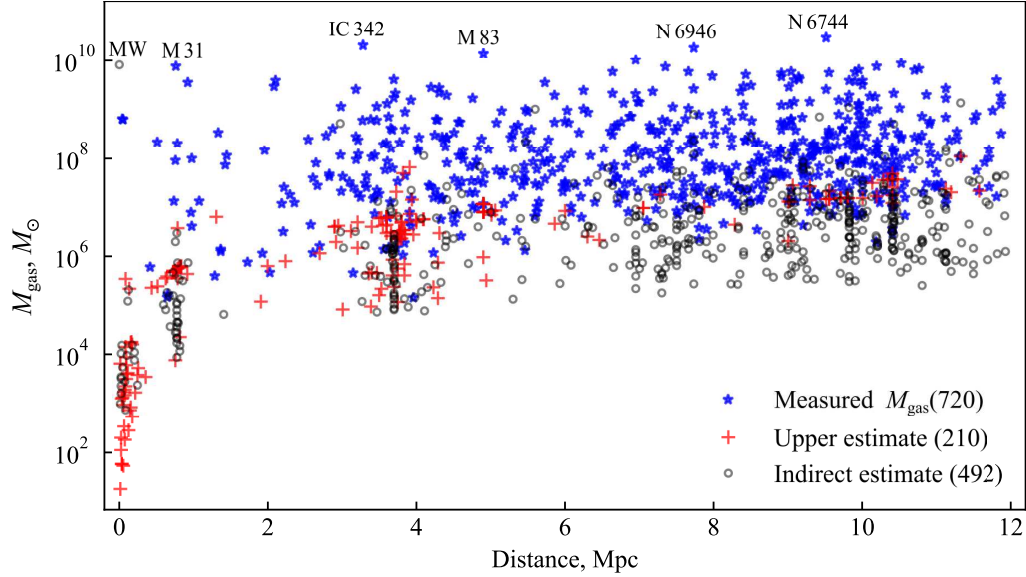


Figure 6. Distribution of the Local Volume galaxies by gas mass and distance. Galaxies with direct M_{gas} estimates are designated by stars, galaxies with upper H I-flux limits are shown by crosses, and galaxies with indirect M_{gas} estimates obtained from calibration dependences are shown by the empty circles.

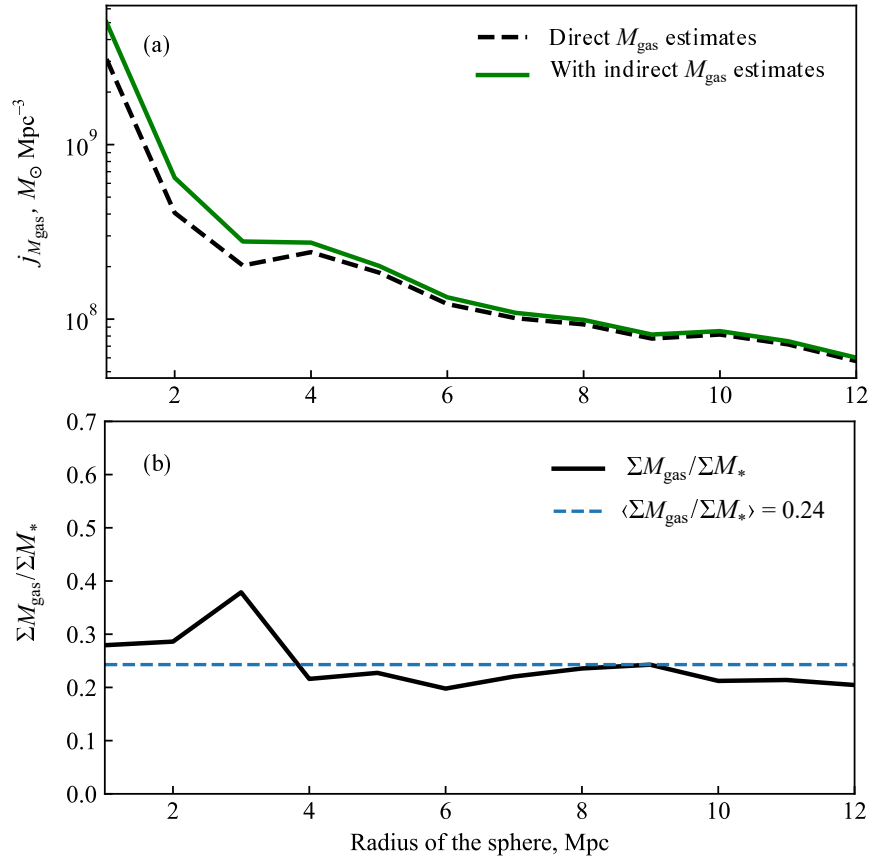


Figure 7. Panel (a)—dependence of the mean gas mass density on distance in the Local Volume. The difference between the upper and lower lines corresponds to the contribution of galaxies with indirect mass estimates, panel (b)—average gas-to-stellar mass ratio in the Local Volume spheres of different radii.

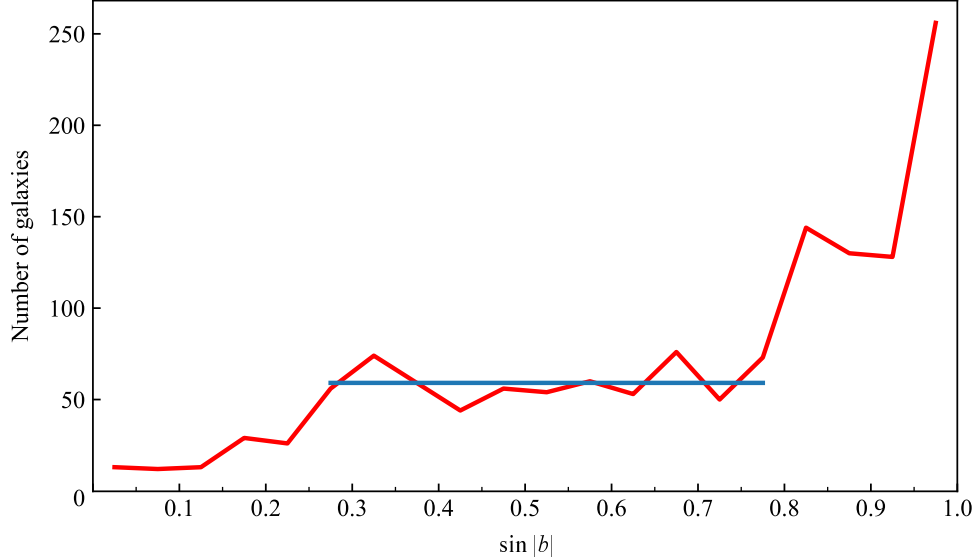


Figure 8. Distribution of the number of Local Volume galaxies in galactic latitude sine intervals with a step of 0.05. The horizontal line corresponds to the assumed values free from the Local supercluster effects and extinction in the Milky Way.

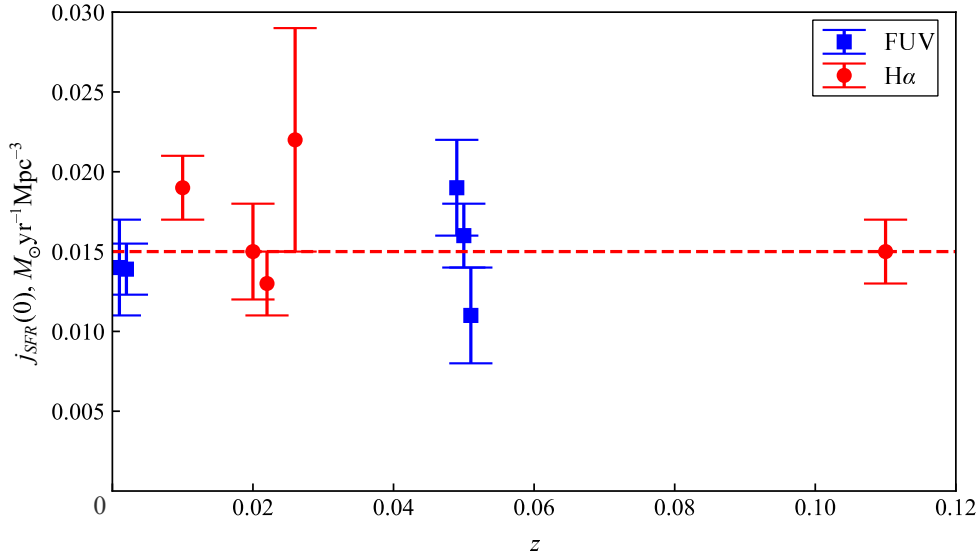


Figure 9. Estimates of global star formation rate per unit Universe volume based on the FUV-flux (squares) and H α -flux (circles) data, reduced to the $z = 0$ epoch, with the Hubble parameter $H_0 = 70 \text{ km s}^{-1} \text{ Mpc}^{-1}$. The horizontal dashed line corresponds to the average value of this quantity according to Madau and Dickinson (2014).

vals of galactic $\sin b$ should be the same. The real distribution of nearby galaxies is distorted by the strong light extinction in the Milky Way zone, as well as by the concentration of galaxies in the Local supercluster plane, which is almost perpendicular to the plane of the Milky Way. Figure 8 shows the distribution of the number

of LV galaxies by $\sin |b|$ intervals with a step of 0.05.

The approximate constancy of the number of galaxies in these intervals is true only at the average galactic latitudes in the $|b| = 15^\circ\text{--}50^\circ$ range. At high latitudes, the excess of the number of galaxies is due to the effect of the Local

supercluster. The expected lack of galaxies at $|b| < 15^\circ$ is caused by the absorption of light by interstellar dust, which is especially strong in the FUV-range. Extrapolating the horizontal line in Fig. 8 to the regions of low galactic latitudes, we derive the shortage in the total number of LV galaxies $\Delta N = 258$. Therefore, the density estimates presented in Fig 4a, should be multiplied by a factor of $(1428 + 258)/1428 = 1.18$. Taking this factor into account, we adopt the average *SFR* density within the distance $D = 11$ Mpc equal to $(1.95 \pm 0.18) \times 10^{-2} M_\odot \text{yr}^{-1} \text{Mpc}^{-3}$. Additionally, since the stellar mass excess in this volume relative to the global value amounts to a factor of 1.46 ± 0.10 (Karachentsev and Telikova, 2018), for the global star formation rate in unit volume we derive the estimate $j_{\text{SFR}} = (1.34 \pm 0.16) 10^{-2} M_\odot \text{yr}^{-1} \text{Mpc}^{-3}$, which is presented in the last column of Table 1.

We should note, however, that the 1.18 factor is obtained in the assumption that the number of unaccounted for galaxies at low galactic latitudes does not depend on their mass (luminosity). This assumption may turn out to be disputable if the percentage of dwarf galaxies obscured from us is significantly higher than that of massive spiral galaxies that contribute the most to the integral star formation rate. Evidently, the effect of this circumstance on the final result is still small.

The mean star formation rate density in the Universe from Table 1 corrected for epoch $z = 0$ is replicated in Fig. 9 with the mean errors indicated. Estimates made from $\text{H}\alpha$ - and FUV-fluxes are shown by, correspondingly, circles and squares. The horizontal dotted line indicates the average value $j_{\text{SFR}}(0) = 0.015 M_\odot \text{yr}^{-1} \text{Mpc}^{-3}$, fixed by Madau and Dickinson (2014) as the most optimal.

Evidently, the $j_{\text{SFR}}(0)$ estimates for $H_0 = 70 \text{ km s}^{-1} \text{Mpc}^{-1}$ and with a correction for the effect of evolution are in good agreement with each other within the margin of measurement error. Systematic differences between the $j_0(\text{SFR})$ values obtained from $\text{H}\alpha$ - and FUV-fluxes are small. The estimates of this value made from infrared galaxy fluxes (Sanders et al., 2003; Takeuchi et al., 2003) also agree with the optical data within errors. We can

assume that at present, the estimates of the cosmic star formation density at $z = 0$ coincide with an accuracy of about 10%.

To conclude, let us note that the analysis and modeling of *SFR* and M_* observational data for the Local Volume galaxies, performed recently by Haslbauer et al. (2023), change noticeably the history of cosmic star formation in the Universe, making the *SFR*(z) dependence more flat and lowering the peak in the Madau diagram for $z \sim 2$ by a factor of 2.2. Haslbauer et al. (2023) used the UNGC catalog data on the average *SFR* and M_* density to test various star formation history models in massive and dwarf galaxies. The authors have shown that the star formation rate evolution model in unit volume, $j_{\text{SFR}}(z)$, with a steep peak at $z \sim 2$, presented by Madau et al. (1998) and Madau and Dickinson (2014), contradicts the observed average stellar mass density in the LV. In order to reconcile the star formation history in the nearby galaxies with the observed amount of their stellar mass, one must assume that the real burst of star formation in the $z \sim 2$ epoch was 2–3 times less intensive than that predicted by the classic Madau diagram.

ACKNOWLEDGMENTS

This work has made use of the Local Volume galaxy database, which is updated with the support of grant No. 075-15-2022-262 (13.MNPMU.21.0003) of the Ministry of Science and Higher Education of the Russian Federation.

REFERENCES

- K. N. Abazajian, J. K. Adelman-McCarthy, M. A. Agüeros, et al., *Astrophys. J. Suppl.* **182** (2), 543 (2009). DOI:10.1088/0067-0049/182/2/543
- G. S. Anand, L. Rizzi, R. B. Tully, et al., *Astron. J.* **162** (2), id. 80 (2021). DOI:10.3847/1538-3881/ac0440
- J. Brinchmann, S. Charlot, S. D. M. White, et al., *Monthly Notices Royal Astron. Soc.* **351** (4), 1151 (2004). DOI:10.1111/j.1365-2966.2004.07881.x

- L. Chomiuk and M. S. Povich, *Astron. J.* **142** (6), article id. 197 (2011). DOI:10.1088/0004-6256/142/6/197
- S. P. Driver, A. S. G. Robotham, L. Kelvin, et al., *Monthly Notices Royal Astron. Soc.* **427** (4), 3244 (2012). DOI:10.1111/j.1365-2966.2012.22036.x
- J. Gallego, J. Zamorano, A. Aragon-Salamanca, and M. Rego, *Astrophys. J.* **455**, L1 (1995). DOI:10.1086/309804
- A. Gil de Paz, S. Boissier, B. F. Madore, et al., *Astrophys. J. Suppl.* **173** (2), 185 (2007). DOI:10.1086/516636
- D. J. Hanish, G. R. Meurer, H. C. Ferguson, et al., *Astrophys. J.* **649** (1), 150 (2006). DOI:10.1086/504681
- M. Haslbauer, P. Kroupa, and T. Jerabkova, *Monthly Notices Royal Astron. Soc.* **524** (3), 3252 (2023). DOI:10.1093/mnras/stad1986
- M. P. Haynes, R. Giovanelli, A. M. Martin, et al., *Astron. J.* **142** (5), article id. 170 (2011). DOI:10.1088/0004-6256/142/5/170
- W. K. Huchtmeier, I. D. Karachentsev, V. E. Karachentseva, and M. Ehle, *Astron. and Astrophys. Suppl.* **141**, 469 (2000). DOI:10.1051/aas:2000324
- P. A. James, J. H. Knapen, N. S. Shane, et al., *Astron. and Astrophys.* **482** (2), 507 (2008). DOI:10.1051/0004-6361:20078560
- T. H. Jarrett, T. Chester, R. Cutri, et al., *Astron. J.* **119** (5), 2498 (2000). DOI:10.1086/301330
- E. I. Kaisina, D. I. Makarov, I. D. Karachentsev, and S. S. Kaisin, *Astrophysical Bulletin* **67** (1), 115 (2012). DOI:10.1134/S1990341312010105
- I. D. Karachentsev and E. I. Kaisina, *Astrophysical Bulletin* **74** (2), 111 (2019). DOI:10.1134/S1990341319020019
- I. D. Karachentsev, V. E. Karachentseva, W. K. Huchtmeier, and D. I. Makarov, *Astron. J.* **127** (4), 2031 (2004). DOI:10.1086/382905
- I. D. Karachentsev, D. I. Makarov, and E. I. Kaisina, *Astron. J.* **145** (4), article id. 101 (2013). DOI:10.1088/0004-6256/145/4/101
- I. D. Karachentsev and K. N. Telikova, *Astronomische Nachrichten* **339** (615), 615 (2018). DOI:10.1002/asna.201813520
- R. C. Kennicutt, Jr., *Annual Rev. Astron. Astrophys.* **36**, 189 (1998). DOI:10.1146/annurev.astro.36.1.189
- B. S. Koribalski, L. Staveley-Smith, V. A. Kilborn, et al., *Astron. J.* **128** (1), 16 (2004). DOI:10.1086/421744
- J. C. Lee, A. Gil de Paz, J. Kennicutt, Robert C., et al., *Astrophys. J. Suppl.* **192** (1), article id. 6 (2011). DOI:10.1088/0067-0049/192/1/6
- J. C. Lee, A. Gil de Paz, C. Tremonti, et al., *Astrophys. J.* **706** (1), 599 (2009a). DOI:10.1088/0004-637X/706/1/599
- J. C. Lee, J. Kennicutt, Robert C., S. J. J. G. Funes, et al., *Astrophys. J.* **692** (2), 1305 (2009b). DOI:10.1088/0004-637X/692/2/1305
- F. Lelli, S. S. McGaugh, and J. M. Schombert, *Astron. J.* **152** (6), article id. 157 (2016). DOI:10.3847/0004-6256/152/6/157
- P. Madau and M. Dickinson, *Annual Rev. Astron. Astrophys.* **52**, 415 (2014). DOI:10.1146/annurev-astro-081811-125615
- P. Madau, L. Pozzetti, and M. Dickinson, *Astrophys. J.* **498** (1), 106 (1998). DOI:10.1086/305523
- D. C. Martin, J. Fanson, D. Schiminovich, et al., *Astrophys. J.* **619** (1), L1 (2005). DOI:10.1086/426387
- P. G. Pérez-González, J. Zamorano, J. Gallego, et al., *Astrophys. J.* **591** (2), 827 (2003). DOI:10.1086/375364
- S. Rahmani, S. Lianou, and P. Barmby, *Monthly Notices Royal Astron. Soc.* **456** (4), 4128 (2016). DOI:10.1093/mnras/stv2951
- M. S. Roberts and M. P. Haynes, *Annual Rev. Astron. Astrophys.* **32**, 115 (1994). DOI:10.1146/annurev.aa.32.090194.000555
- A. S. G. Robotham and S. P. Driver, *Monthly Notices Royal Astron. Soc.* **413** (4), 2570 (2011). DOI:10.1111/j.1365-2966.2011.18327.x
- S. Salim, R. M. Rich, S. Charlot, et al., *Astrophys. J. Suppl.* **173** (2), 267 (2007). DOI:10.1086/519218
- D. B. Sanders, J. M. Mazzarella, D. C. Kim, et al., *Astron. J.* **126** (4), 1607 (2003). DOI:10.1086/376841
- M. F. Skrutskie, R. M. Cutri, R. Stiening, et al., *Astron. J.* **131** (2), 1163 (2006). DOI:10.1086/498708
- T. T. Takeuchi, K. Yoshikawa, and T. T. Ishii, *Astrophys. J.* **587** (2), L89 (2003). DOI:10.1086/375181
- T. K. Wyder, M. A. Treyer, B. Milliand, et al., *Astrophys. J.* **619** (1), L15 (2005). DOI:10.1086/424735
- R. Zhou, M. Zhu, Y. Yang, et al., *Astrophys. J.* **952** (2), id. 130 (2023). DOI:10.3847/1538-4357/acdcf5